Differential and common-mode filters based on metamaterial resonators

Ignacio Gil* and Raúl Fernández-García
Department of Electronic Engineering
Universitat Politècnica de Catalunya
Colom 1, 08222 Terrassa, Spain
*e-mail: ignasi.gil@upc.edu

***Abstract*—Two different techniques based on metamaterials for mitigating both the differential and common-mode propagation in differential signaling are addressed. The proposed filters are implemented by means of complementary split ring and spiral resonators applied to coupled parallel microstrip lines. Frequency response, signal integrity and radiation emission are analyzed.**

Keywords—Differential-mode filter; common-mode filter, electromagnetic interference, complementary split ring resonator, metamaterial.

I. INTRODUCTION

Differential signaling provides, theoretically, high immunity to noise and crosstalk as well as a low level of radiated electromagnetic interference (EMI). In practical applications, small asymmetries caused by traces length, time skew or imbalances in the two transmitted signals generate the conversion of some of the differential-mode (DM) signal to common-mode (CM) which can be critical in the electromagnetic compatibility (EMC) performance of high data-rate transmission for high-speed digital electronic buses and circuits. In order to overcome this issue, some compact common-mode filters based on metamaterials such as electromagnetic bandgap (EBGs) [1] or negative-permittivity metamaterials [2] have been presented.

Complementary split-ring resonators (CSRRs) are used to implement a type of metamaterials, the so-called single negative effective media (SNG) with electric permittivity, $\varepsilon<0$ [3]. CSRRs consist of two concentric split rings with opposite cuts etched in a ground plane (Fig. 1a) and they are excited by an applied electric field, parallel to the CSRRs axis. Those electrical resonance properties have been applied in recent works to mitigate simultaneous switching noise propagation in high-speed printed circuits boards (PCBs) [4] and to reduce the EMI susceptibility of in small signal analog circuits [5]. In addition, CSRRs constitute sub-wavelength resonators and, therefore, they present lower dimensions with regard to EBGs [6]. Alternatively, other SNG can be implemented with particles such as complementary spiral resonators (CSRs). Fig. 1b shows the topology of a CSR whose resonance frequency, $f_{0,\,CSR}$ roughly arises at $f_{0,\,CSRR}/2$ as stated at [7] and, therefore, it can be used to miniaturize a given CSRR structure in a factor 2. Recently, a first approach of common-mode filter based on CSRRs has been presented for Ethernet LAN applications [8].

This work was supported by the Spanish Government-MINECO under Project TEC2010-18550 and AGAUR 2009 SGR 1425.

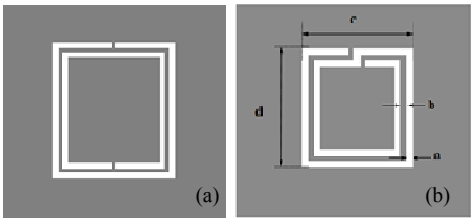

Fig. 1. (a) Topology of the CSRR and the (b) CSR with its relevant dimensions. Metallization zones are depicted in grey.

In this paper, the analysis of both differential and common-mode filters for parallel coupled microstrip line based on CSRRs and CSRs sub-wavelength resonators is addressed. Electromagnetic simulation and experimental validation of the differential and common-mode filters are reported, as well as the signal integrity performance for all the considered cases. Moreover, the impact in terms of radiated emission due to the alteration of the solid ground plane (due to the presence of the etched resonators) has been investigated by carrying out an electric far-field analysis.

The paper is organized as follows. Section II discusses the CSRR and CSR differential and common-mode layout topologies and equivalent circuit models. The frequency response of the proposed structures is simulated and tested by means of a differential S-parameter analysis in Section III. Signal integrity performance is also evaluated in Section III. EMI radiation is studied and discussed in section IV. Finally, the main conclusions are drawn and summarized in Section V.

II. DIFFERENTIAL AND COMMON-MODE METAMATERIAL FILTERS BASED ON CSRRS AND CSRS

A. CSRR- and CSR-CM-DM filters

Fig. 2 illustrates the unit cell topology of a CSRR-CM-DM (common- and differential-mode rejection) filter as well as its distributed equivalent circuit model. Each CSRR is electrically coupled with one microstrip line by means of the capacitance C. L models the self-inductance of the lines, whereas C_C and L_C constitute the parallel resonant tank corresponding to the CSRRs. The mutual capacitance (crosstalk) is modeled by C_m and the mutual inductance between transmission lines has been neglected for simplicity. All parameters are considered per-unit-length elements. The same lumped model is achieved by etching CSRs in the ground plane instead of CSRRs. If we

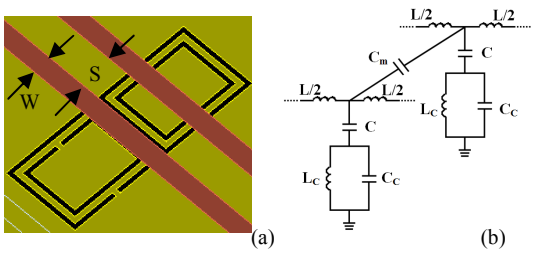

Fig. 2. (a) CSRR-CM-DM unit cell topology and (b) distributed circuit model.

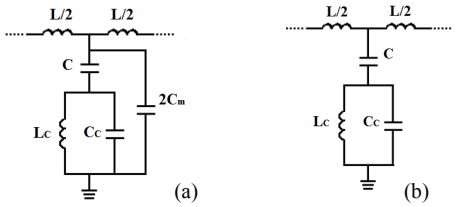

Fig. 3. Distributed circuit models for the: (a) differential (odd) mode and (b) common (even) mode.

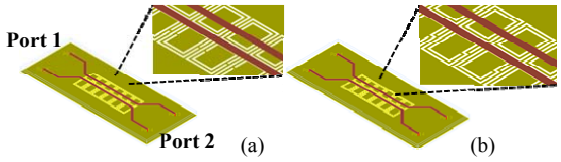

Fig. 4. Configuration of the proposed structure for: (a) 6-stage CSRR-CM-DM filter and (b) 6-stage CSR-CM-DM filter.

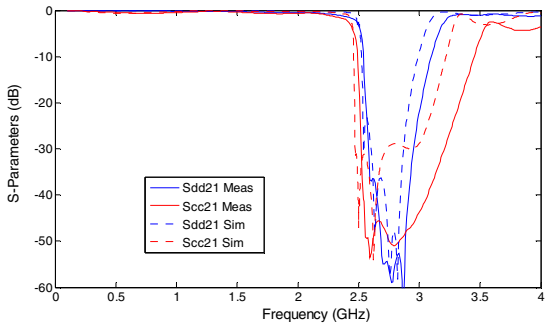

Fig. 5. Common-mode and differential-mode S-parameters for the CSRR-CM-DM proposed topology.

analyze the differential (odd) and common (even) modes, the equivalent circuits results in models depicted in Fig. 3. In both cases a parallel notch resonance arises and, therefore, a stop-band frequency response is expected for both differential and common modes. Notice that the expected notch center frequency is very similar for both propagation modes, since the capacitance C_m has a low impact with regard to the other circuit elements. To verify this behavior three prototypes have been electromagnetically simulated and tested. Fig. 4 shows the prototype setup consisting of 4-port 6-stage CSRR and CSR loaded parallel transmission lines, designed to obtain a stop band filter around 2.5 GHz and 1.3 GHz, respectively. The substrate corresponds to the commercial *Rogers* RO3010 (dielectric constant ε_r=10.2, thickness h=1.27 mm). Specifically, 50 Ω microstrip lines are considered whose dimensions are: width W=1.18 mm, length l=32.9 mm, and separation, s=2.1 mm. 45º access lines have been added for convenience in order to insert the port connectors. CSRRs and CSRs dimensions correspond to a=b=0.3 mm c=6.27 mm, and d=5 mm. Fig. 5 shows the comparison between electromagnetic simulations performed with the *Agilent Momentum* software and the experimental S-parameter results for the CSRR-CM-DM filters. As expected, both propagation modes are cancelled, and similar rejection level is achieved, about 50 dB. Notice that the rejection frequency band in the case of common-mode is significantly enhanced with regard to the differential mode. Although the electromagnetic simulation includes second order effects such as tolerances in the fabrication process, a slight underestimation of the frequency band is observed.

B. CSRR- and CSR-CM filters

An interesting application consists of attenuating the common-mode signal interference whereas preserving the differential-mode. This possibility is achieved by etching either CSRRs or CSRs underneath the microstrip coupled lines in the way shown in Fig. 6a. The corresponding equivalent circuit is depicted in Fig. 6b. As can be seen, each sub-wavelength resonator is electrically coupled simultaneously to both coupled lines. By developing the distributed equivalent circuits for the odd and even modes, the models illustrated in Fig. 7 are obtained. In this case, only the common-mode is rejected due to the resonance behavior due to the presence of the CSRRs or CSRs. Notice that the differential-mode is normally propagated, since the circuit model corresponds to a conventional transmission line with an increased per-section capacitance. Again, two CSRR- and CSR-CM prototypes have been simulated and tested. Figs. 8 and 9 illustrate the described behavior with a rejection level for the common-mode in the order of 50 dB and 40 dB, respectively. Since the dimensions of CSRRs and CSRs are equivalent, the resonance of the latter arises at a half of the corresponding to CSRRs particles. However, CSRRs show a better behavior in terms of rejection bandwidth.

III. SIGNAL INTEGRITY PERFORMANCE

In this section, the signal integrity of the presented structures is investigated by means of the standard eye diagram metric. Two parameters have been considered as metric of the eye pattern quality, the maximum eye width (MEW) and the maximum eye height (MEH). A cosimulation of the eye diagram has been performed by using a time-domain pseudo-random bit sequence coded at 2 GHz as the input excitation of the corresponding design layouts. The transmitted bit-sequence swing corresponds to a 600 mV differential signal with a 0.2 ns nominal rise/fall time. Table I summarizes the obtained results and the comparison with the reference microstrip coupling lines case (solid ground plane). It is found that the impact of the common-mode metamaterial topologies in terms of signal integrity performance is negligible. In fact, the signal integrity degradation caused by the CSRR-CM topology is only about 0.2% for the eye width and effectively

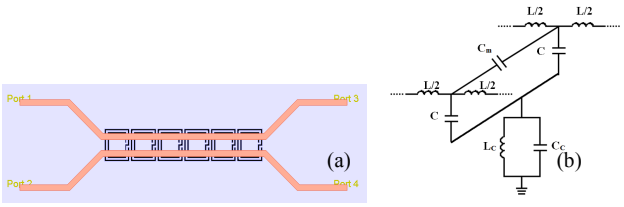

Fig. 6. (a) CSR-CM prototype and (b) unit cell distributed circuit model.

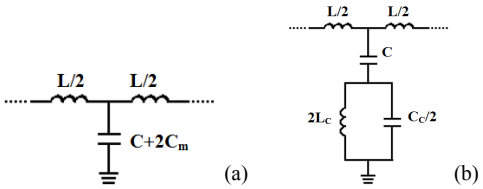

Fig. 7. Distributed circuit models for the: (a) differential (odd) mode and (b) common (even) mode.

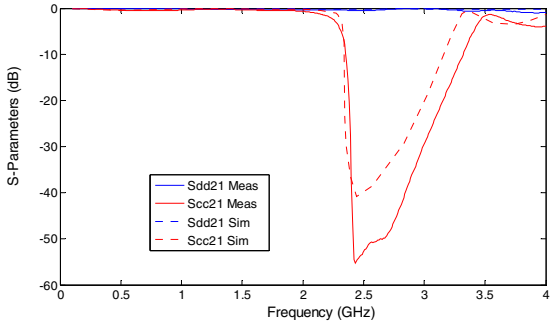

Fig. 8. Common-mode and differential-mode S-parameters for the CSRR-CM proposed topology.

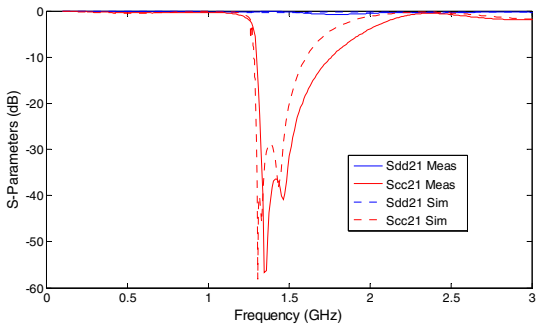

Fig. 9. Common-mode and differential-mode S-parameters for the CSR-CM proposed topology.

null for the eye height, whereas the CSR-CM topology degradation correspond to 0.6% and 0.4%, respectively. Concerning the common and differential-mode topologies, a significant degradation is observed. The CSRR-CM-DM filter degrades MEW a 6.6% and MEO a 4.4%. The worst case

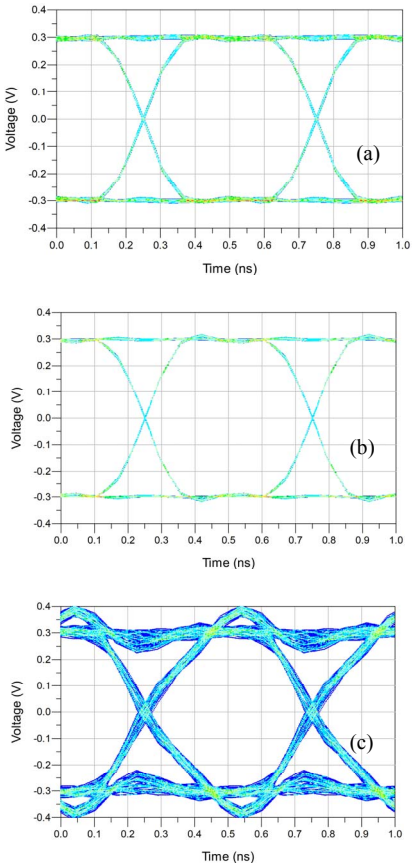

Fig. 10. Eye diagrams generated. (a) Reference case, (b) CSRR-CM filter case and (c) CSRR-CM-DM filter case.

corresponds to the CSR-CM-DM with a degradation of 16.7% for the eye width and 59.8% for the eye height.

TABLE I. SUMMARY OF SIGNAL INTEGRITY PERFORMANCE

Table Column Head		
Implementation	**MEW (ps)**	**MEO (mV)**
Reference	498	569
CSRR-CM	497	569
CSRR-CM-DM	465	544
CSR-CM	495	567
CSR-CM-DM	415	229

IV. RADIATED EMISSION

The effect of etching CSRRs and CSRs on the ground plane has been analyzed in terms of the radiated emission in comparison with conventional electromagnetic coupled parallel signal traces. The far-field radiated emissions of the implementations detailed in Section II have been simulated by using the *Agilent Momentum* software. A differential excitation source of 0 dBm has been applied with all ports matched (Z_p=50 Ω). The normalized radiation pattern has been considered with regard to the maximum radiated

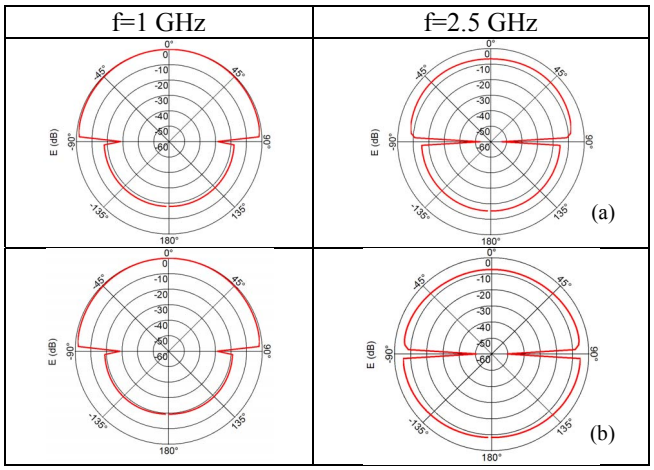

Fig. 11. Normalized radiation pattern for □=90º at 1 GHz and 2.5 GHz. (a) CSRR-CM filter, (b) CSRR-CM-DM filter.

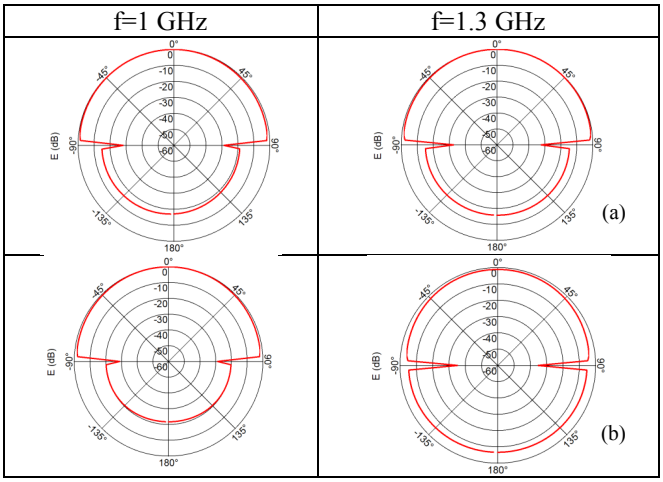

Fig. 12. Normalized radiation pattern for □=90º at 1 GHz and 1.3 GHz. (a) CSR-CM filter, (b) CSR-CM-DM filter.

electromagnetic field, E_{max}, which has been calculated by taking into account the maximum electric field components in both □ and θ coordinates, $E_{□,max}$, and $E_{\theta,max}$, according to:

$$E_{max} = \sqrt{\left(E_{\phi,max}\right)^2 + \left(E_{\theta,max}\right)^2}. \quad (1)$$

Fig. 11 depicts the radiation pattern results of the CSRR-CM-DM and CSRR-CM filter for the observation yz plane (ϕ=90º), which allows to visualize their radiation impact. Two single frequencies have been considered. As can be seen at *f*=1 GHz (outside the resonance region of the CSRRs) the radiation pattern is similar for both structures. However, in the filter's stop-band range (*i.e.*, *f*=2.5 GHz) an increased level of radiation of 6.9 dB is observed for the CSRR-CM-DM filter at the observation point θ=180º. This level corresponds to 8.4 dB for θ=135º. Similar results are achieved for the case of CSR-CM-DM and CSR-CM filters. In this case, radiation patterns are compared at 1 and 1.3 GHz (see Fig. 12). At θ=180º a difference of 9.1 dB is obtained between the radiation level of both filters at 1.3 GHz, whereas at θ=135º the difference is 9.8 dB. Therefore, a significant increasing on the radiation pattern is observed for the -CM-DM configurations due to the higher number of etched rings and the absorption of the conducted differential mode. Moreover, the maximum electric field has been analyzed in order to determine the different impact in terms of the corresponding single negative media. The analysis reveals that the CSRR-CM filter presents the lower level of radiation (with an average value 11 dB higher than the conventional reference case). This value is increased up to 12 dB in the CSR-CM filter case. Both CSRR and CSR-CM-DM present a level of radiation 18 dB higher than the conventional coupled transmission lines. According to these results, the best choice in terms of radiation corresponds to the CSRR particles in order to implement common-mode metamaterials filters. However, a tradeoff appears in terms of radiation level-area, since CSR particles are more suitable in order to obtain compact implementations at the same operation frequency.

V. CONCLUSION

Two design strategies for filtering differential and common-mode propagation based on SNG metamaterials are presented and discussed. A good agreement between electromagnetic simulation and experimental frequency response is achieved in all cases with rejection levels up to 50 dB. According to the signal integrity and radiated emission analysis, a tradeoff between CSRRs and CSRs particles in terms of area-performance appears. CSRRs present a higher bandwidth rejection, lower impact in terms of signal integrity and far-field emission, whereas CSRs achieve more compact implementations due to their resonance properties.

REFERENCES

[1] F. de Paulis, L. Raimondo, S. Connor, B. Archambeault and A. Orlandi, "Compact configuration for common mode filter design based on planar electromagnetic bandgap structures", IEEE Trans. on Electromagnetic Compatibility, vol. 54, pp. 646-654, June 2012.

[2] C.-H. Tsai and T.-L. Wu, "A broadband and miniaturized common-mode filter for gigahertz differential signals based on negative-permittivity metamaterials", IEEE Trans. on Microwave Theory and Techniques, vol. 58 pp. 195-202, January 2010.

[3] F. Falcone, T. Lopetegi, J.D. Baena, E. Marqués, F. Martín and M. Sorolla, "Effective negative- ε stop-band microstrip lines based on complementary split ring resonators", IEEE Microwave and Wireless Component Letters, vol. 14, pp. 280–282, June 2004.

[4] M. M. Bait-Suwailam and O. M. Ramahi, "Ultrawideband mitigation of simultaneus switching noise and EMI reduction in high-speed PCBs using complementary split-ring resonators", IEEE Trans. on Electromagnetic Compatibility, vol. 54, pp. 389-396, April 2012.

[5] D. Pérez, I. Gil, J. Gago, R. Fernández, J. Balcells, D. González, N. Berbel and J. Mon, "Reduction of EMI susceptibility in circuits based on operational amplifiers using complementary split-ring resonators", IEEE Trans. on Components, Packaging and Manufacturing Technology, vol. 2, pp. 240-247 February 2012.

[6] I. Gil and R. Fernández, "Comparison between complementary split ring resonators and electromagnetic band-gap as EMI reduction structures", International Symposium on EMC Europe 2010, Wroclaw, Poland, September 2010.

[7] J.D. Baena, J. Bonache, F. Martín, R. Marqués, F. Falcone, T. Lopetegui, M.A.G. Laso, J. García-García, I. Gil, M. Flores Portillo and M. Sorolla. "Equivalent-circuit models for split-ring resonators and complementary split-ring resonators coupled to planar transmission lines", IEEE Trans. on Microwave Theory and Techniques, vol. 53, pp. 1451-1461, April 2005.

[8] A. Pachon, F. Silva, "Ethernet 10GBASE-T common mode filter based on metamaterial", International Symposium on EMC Europe 2011, UK, September 2011.